Molecular Phylogenetics and Evolution 166 (2022) 107332

Contents lists available at ScienceDirect

Molecular Phylogenetics and Evolution

journal homepage: www.elsevier.com/locate/ympev

Homoploid hybrids, allopolyploids, and high ploidy levels characterize the evolutionary history of a western North American quillwort (*Isoëtes*) complex

Jacob S. Suissa [a,b,c,*], Sylvia P. Kinosian [d], Peter W. Schafran [c,e], Jay F. Bolin [f], W. Carl Taylor [c], Elizabeth A. Zimmer [c]

[a] The Department of Organismic and Evolutionary Biology, Harvard University, Cambridge, MA, USA
[b] The Arnold Arboretum of Harvard University, Boston, MA, USA
[c] Department of Botany, National Museum of Natural History, Smithsonian Institution, Washington, DC, USA
[d] Department of Biology & Ecology Center, Utah State University, Logan, UT, USA
[e] Boyce Thompson Institute, Ithaca, NY, USA
[f] Department of Biology, Catawba College, Salisbury, NC, USA

ARTICLE INFO

Keywords:
Hybrid
Lycophytes
Polyploid
RADseq
Reticulation
Speciation

ABSTRACT

Polyploidy and hybridization are important processes in seed-free plant evolution. However, a major gap lies in our understanding of how these processes affect the evolutionary history of high-ploidy systems. The heterosporous lycophyte genus *Isoëtes* is a lineage with many putative hybrids and high-level polyploid taxa (ranging from tetraploid to dodecaploid). Here, we use a complex of western North American *Isoëtes*, to understand the role of hybridization and high-level polyploidy in generating and maintaining novel diversity. To uncover these processes, we use restriction-site associated DNA sequencing (RADseq), multiple alleles of a single low-copy nuclear marker, whole plastomes, cytology (genome size estimates and chromosome counts), and reproductive status (fertile or sterile). With this dataset, we show that hybridization occurs easily between species in this complex and is bidirectional between identical, but not different, cytotypes. Furthermore, we show that fertile allopolyploids appear to have formed repeatedly from sterile homoploid and interploid hybrids. We propose that low prezygotic reproductive barriers and a high frequency of whole-genome duplication allow for high-level polyploid systems to generate novel lineages, and that these mechanisms may be important in shaping extant *Isoëtes* diversity.

1. Introduction

Across many lineages, interspecies hybridization has led to evolutionary histories that are better explained through reticulating, rather than bifurcating, branches on a phylogenetic tree (Edelman et al., 2019; Linder and Rieseberg, 2004; Nakhleh et al., 2005; Soltis and Soltis, 2000). Hybridization coupled with polyploidization (genome doubling) is important because it can lead to the generation and maintenance of novel lineages. These lineages form the basis for reticulate species complexes, which are webs of related taxa typically involving multiple parental species, sterile (or partially sterile) interspecific hybrids (Dobzhansky, 1982), and fertile auto- or allopolyploids (i.e., products of genome duplication with one or more parental genomes, respectively; Grant, 1971; Rieseberg, 1997; Stebbins, 1969). Sterile hybrids within these complexes are sometimes considered evolutionary dead ends, but through allopolyploidization, fertility can be restored because each chromosome will have a match in its newly duplicated genome (Soltis and Soltis, 2000; Stebbins, 1947; Wagner and Wagner, 1980). In addition, allopolyploidy can lead to fixed genomic variation (homeologous heterozygosity; Klekowski, 1976) allowing for low inbreeding depression following self-fertilization in fertile allopolyploids (Haufler et al., 2016; Husband et al., 2008; Soltis et al., 2014; Soltis and Soltis, 2000). For these reasons, allopolyploidy is suggested to be evolutionarily advantageous within certain lineages—however, the importance of this process as a broader driver of diversification is debated (Landis et al., 2018; Mayrose et al., 2015, 2011; Soltis et al., 2014).

* Corresponding author at: 1300 Centre St. Jamaica Plain, MS 02131, USA.
E-mail address: jsuissa@g.harvard.edu (J.S. Suissa).

https://doi.org/10.1016/j.ympev.2021.107332
Received 15 February 2021; Received in revised form 5 October 2021; Accepted 18 October 2021
Available online 20 October 2021

Reticulate species complexes are common in plants (Burnier et al., 2009; Nauheimer et al., 2019; Sandstedt et al., 2020), especially in seed-free vascular plants (ferns and lycophytes; Barrington et al., 1989; Sigel, 2016; Wood et al., 2009). Among ferns and lycophytes, most studies have focused on homosporous ferns, with less work on the homo- or heterosporous lycophytes. In particular, the heterosporous genus *Isoëtes* L. (Isoetaceae) is of evolutionary interest because reticulate species complexes that contain high-level polyploids are widespread in the genus (Britton and Brunton, 1989; Brunton and Britton, 2000; Hickey et al., 1989; Pereira et al., 2018; Small and Hickey, 2001; Taylor and Hickey, 1992; Taylor and Luebke, 1988). Moreover, *Isoëtes* is a cosmopolitan genus comprising 250–350 species, ~60% of which are polyploid (Troia et al., 2016). The genus has also been described as a "living fossil" for its morphological stasis, and it is the last remaining lineage of the ancient isoetalean lycopsids—a clade that dates back to the middle Devonian (~400 mya; Pigg, 1992). However, most of the extant diversity is relatively young (~60–150 mya; Larsén and Rydin, 2016; Wood et al., 2020) where hybridization and polyploidization may have played an important role in generating novel lineages (Dai et al., 2020; Hoot et al., 2004; Taylor and Hickey, 1992). *Isoëtes* is an ideal study system for investigating the evolutionary implications of hybridization and high-level polyploidy within vascular plants because of its unique evolutionary dynamics (i.e., an old lineage with recent diversification), species richness, pervasiveness of polyploids with high ploidy, and complex biogeographical patterns (*e.g.*, global distributions, disjunct populations, and putative long-distance dispersal).

Although there is great potential for investigating reticulate evolution within *Isoëtes*, discerning species relationships in the genus has historically proven difficult due to the conserved body plan with limited morphological characters and character states, combined with high intraspecific variation (Freund et al., 2018; Hickey et al., 1989; Pfeiffer, 1922). In fact, early Isoetologist W. N. Clute (1905) lamented, *"the marks by which the species [of* Isoëtes*] are distinguished are so obscure as to be puzzling to all but the select few, and in consequence the species have been largely taken upon by faith."* Recent work demonstrated that low molecular divergence further compounds the difficulties of classifying species within this genus (Pereira et al., 2017; Wood et al., 2020).

One species complex of *Isoëtes* ripe for investigation is known from western North America. This complex putatively includes two diploid progenitors (*I. echinospora* Durieu and *I. bolanderi* Engelm.), a sterile diploid hybrid (*I.* × *herb-wagneri* W. C. Taylor), a fertile allotetraploid (*I. maritima* Underwood), fertile hexaploid (*I. occidentalis* L. F. Hend.), and a couple of sterile interploid hybrids (the triploid *I.* × *pseudotruncata* D. M. Britton & D. F. Brunt. and the pentaploid *I.* × *truncata* Clute; Figs. 1, 2a). The evolutionary relationships among taxa in this complex have been suggested before using morphology and cytology, but a consensus has yet to be reached (Fig. 1; Britton et al., 1999; Britton and Brunton, 1996, 1993; Taylor, 2002).

Here, we revisit this complex using phylogenomic data with the specific intention of investigating the evolutionary implications of polyploidy and hybridization within this high-ploidy system. We leverage multiple distinct data sets to accomplish this: restriction-site associated DNA sequencing (RADseq), alleles of a low-copy nuclear marker, whole plastomes, cytology, and reproductive status. With these data, we were able to reconstruct the reticulate evolutionary history and directionality of hybridization events, as well as ploidy and fertility status of hybrid taxa, taking a step towards understanding the evolutionary dynamics within the genus. These data provide additional support that hybridization and polyploidy occur in the genus and that allopolyploidy—and potentially autopolyploidy—may be important evolutionary processes shaping extant *Isoëtes* diversity.

2. Materials and methods

We generated five datasets to investigate the hybridization and polyploidy in a reticulate complex of western North American *Isoëtes*. We performed flow cytometry to estimate genome size; utilized Illumina short-read double digest RADseq to obtain genomic data for population structure analysis and phylogenetic network analysis; identified fertility vs. sterility in spores; sequenced whole chloroplasts with Illumina; and sequenced all copies of the *LFY* nuclear marker within diploids and hybrid polyploid species using the Pacific Biosciences (PacBio) long-read platform.

2.1. Taxon sampling

Within each dataset collections from various sources were utilized (Table 1). For RADseq and cytology, we collected fresh and silica-dried leaf tissue from localities across western North America (Fig. 2a). These included high-elevation lakes in Montana, California, and British Columbia. To determine specimen fertility, we examined spores from these collections. Specimen information for each sample can be found in (Table 1). While the species were the same, the samples for plastome and *LFY* allele sequencing did not fully overlap with those that we used for RADseq (Table 1).

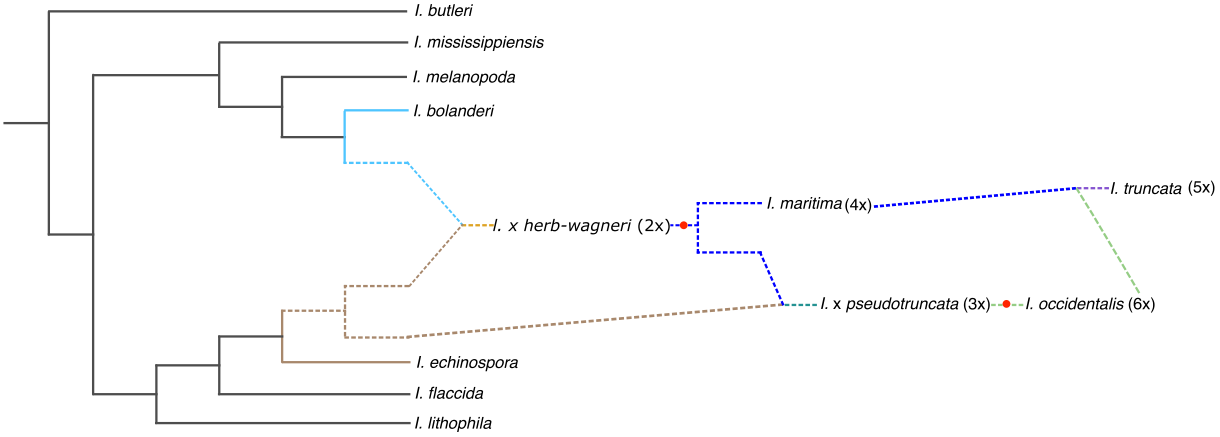

Fig. 1. Historically hypothesized relationships of western North American *Isoëtes*, derived from Britton & Brunton, 1993, 1996; Britton et al., 1999; and Taylor, 2002. It was hypothesized that *Isoëtes bolanderi* and *I. echinospora* hybridize to form the sterile diploid *I.* × *herb-wagneri*. *Isoëtes maritima* is formed via a whole genome duplication (WGD; indicated by red dot) of *I.* × *herb-wagneri*. *Isoëtes maritima* (2x gamete) hybridizes with *I. echinospora* (1x gamete) to form triploid *I.* × *pseudotruncata*. The triploid goes through a WGD (red dot) to form *I. occidentalis*. Finally, it was hypothesized that *I. maritima* (2x gamete) and *I. occidentalis* (3x gamete) hybridize to form the pentaploid *I. truncata*. (For interpretation of the references to color in this figure legend, the reader is referred to the web version of this article.)

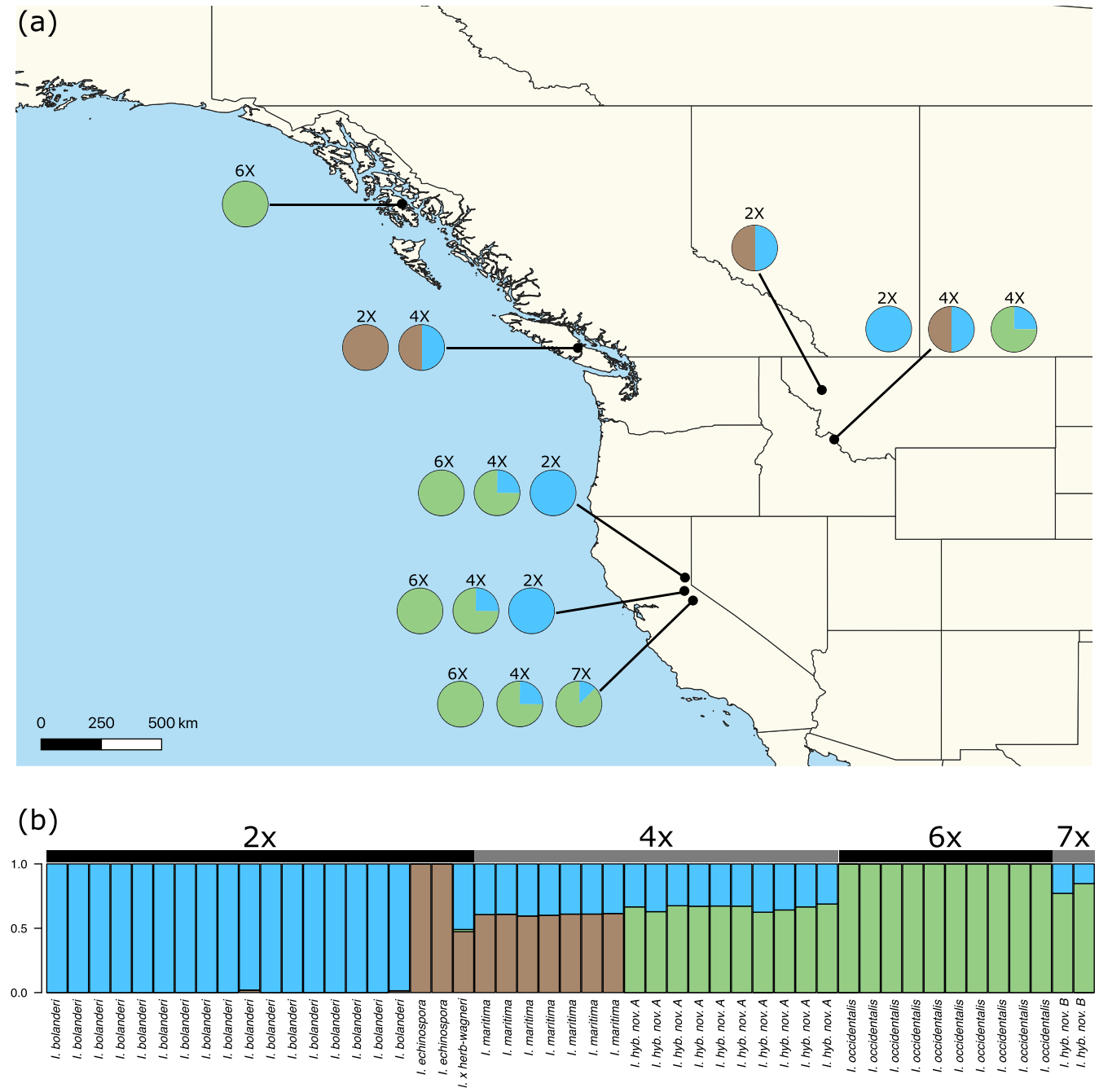

Fig. 2. Sampling locations and population structure ($K = 3$) of western North American *Isoëtes*; (a) points represent lake localities where species were collected, pie charts indicate the genomic structure of different individuals collected at each location and the numbers above the pie charts indicate ploidy. The ploidy was derived from C-values or chromosome counts and the genomic constitution was derived from the STRUCTURE analysis; (b) population structure and ploidy level for each sample; the diploid species (*I. bolanderi*, blue; *I. echinospora*, brown) and hexaploid *I. occidentalis* (green) are separated as the three main species with distinct genomic populations. Colors in the pie charts on the map correspond with the genomic constitutions derived from STRUCTURE. (For interpretation of the references to color in this figure legend, the reader is referred to the web version of this article.)

2.2. Inferring ploidy

Fresh leaf material was used to measure C-values for individuals of each taxon in order to estimate their ploidy. A C-value measures the haploid DNA content (in picograms) in an organism. C-values were estimated using microphylls (leaves) from living plants. Leaves were prepared for DNA flow cytometry as described in Bolin et al., 2017 using propidium iodide stain (P121493; Molecular Probes FluoroPure, ThermoFisher Scientific, Waltham, Massachusetts, USA). Newly expanded leaves of the *Glycine* max 'Polanka' (Doležel et al., 1994) were used as the standard for genome size estimation; 1C = 1.25. Samples were run together with the standard and were analyzed with a BD Accuri C6 Flow Cytometer and associated software (Becton Dickinson and Company, Franklin Lakes, New Jersey, USA), using gating and peak estimation parameters described in Bolin et al., (2017). C-values were calculated for each individual following the methods of Dolezel and Bartos, (2005). All C-values reported here are 1C, as defined by Greilhuber et al., (2005). By measuring the C-value for specimens identified as species with well-documented chromosome counts, we were able to infer ploidy levels for individual plants using C-value estimates. This included *I. bolanderi*,

Table 1
This table consists of individuals used in the RADseq, plastome, and *LFY* sequencing. It contains information on the individual collection numbers, locality, 1C-values (based on flow cytometry), and inferred ploidy levels. If samples do not have 1C-values but have an inferred ploidy, this means that chromosome counts through root tip squashes were made for these individuals. Collector names are as follows: JSS – Jacob S. Suissa; WCT – W. Carl Taylor; PWS – Peter W. Schafran.

Taxon	Collector	Collector Number	Locality	Lake	Latitude	Longitude	1C-value	Inferred ploidy	Sequencing type
I. bolanderi	WCT	6754	California	Tamarack lake	38.8481	−120.1	NA	2x	RADseq/Plastome
I. bolanderi	JSS	300_a	Montana	Twin lakes	45.41283	−113.7	2.47	2x	RADseq
I. bolanderi	JSS	300_b	Montana	Twin lakes	45.41283	−113.7	2.46	2x	RADseq
I. bolanderi	JSS	300_c	Montana	Twin lakes	45.41283	−113.7	2.62	2x	RADseq
I. bolanderi	JSS	300_d	Montana	Twin lakes	45.41283	−113.7	2.51	2x	RADseq
I. bolanderi	JSS	300_e	Montana	Twin lakes	45.41283	−113.7	2.47	2x	RADseq
I. bolanderi	JSS	300_f	Montana	Twin lakes	45.41283	−113.7	2.57	2x	RADseq
I. bolanderi	JSS	300_g	Montana	Twin lakes	45.41283	−113.7	2.7	2x	RADseq
I. bolanderi	JSS	300_h	Montana	Twin lakes	45.41283	−113.7	2.58	2x	RADseq
I. bolanderi	JSS	300_i	Montana	Twin lakes	45.41283	−113.7	2.59	2x	RADseq
I. bolanderi	JSS	300_j	Montana	Twin lakes	45.41283	−113.7	2.41	2x	RADseq
I. bolanderi	JSS	300_k	Montana	Twin lakes	45.41283	−113.7	2.53	2x	RADseq
I. bolanderi	JSS	328_a	California	Tamarack lake	38.84517	−120.097	2.6	2x	RADseq
I. bolanderi	JSS	328_b	California	Tamarack lake	38.84517	−120.097	2.64	2x	RADseq
I. bolanderi	JSS	330_a	California	Eagle Lake	38.94315	−120.123	2.4	2x	RADseq
I. bolanderi	JSS	330_b	California	Eagle Lake	38.94315	−120.123	2.5	2x	RADseq
I. bolanderi	JSS	330_c	California	Eagle Lake	38.94315	−120.123	2.4	2x	RADseq
I. echinospora	PWS	32	New York	Cleveland lake	43.79837	−75.2794	NA	2x	RADseq
I. echinospora	JSS	313	British Columbia	Comox lake	49.57446	−125.185	3.97	2x	RADseq
I. × herbwagneri	WCT	6989–3	British Columbia	Comox lake	49.57446	−125.185	NA	2x	LFY/Plastome
I. echinospora	WCT	6989–1	British Columbia	Comox lake	49.57446	−125.185	NA	2x	LFY
I. echinospora	WCT	6991–2	British Columbia	Comox lake	49.57446	−125.185	NA	2x	LFY
I. × herbwagneri	WCT	6991–1	British Columbia	Comox lake	49.57446	−125.185	NA	2x	LFY/Plastome
I. × herbwagneri	WCT	7156	Montana	Twin lakes	45.41283	−113.7	NA	2x	RADseq
I. maritima	WCT	6983	British Columbia	Somas river	49.14237	−124.794	NA	4x	LFY/Plastome
I. maritima	WCT	6987	British Columbia	Comox lake	49.57446	−125.185	NA	4x	LFY
I. maritima	WCT	6990	British Columbia	Comox lake	49.57446	−125.185	NA	4x	LFY/Plastome
I. maritima	JSS	314_a	British Columbia	Comox lake	49.57446	−125.185	6.42	4x	RADseq
I. maritima	JSS	314_b	British Columbia	Comox lake	49.57446	−125.185	6.43	4x	RADseq
I. maritima	JSS	314_c	British Columbia	Comox lake	49.57446	−125.185	6.08	4x	RADseq
I. maritima	JSS	314_d	British Columbia	Comox lake	49.57446	−125.185	6.33	4x	RADseq
I. maritima	JSS	314_e	British Columbia	Comox lake	49.57446	−125.185	6.36	4x	RADseq
I. maritima	JSS	314_f	British Columbia	Comox lake	49.57446	−125.185	6.29	4x	RADseq
I. maritima	JSS	314_G	British Columbia	Comox lake	49.57446	−125.185	NA	NA	RADseq
I. occidentalis	WCT	6755	California	Tamarack lake	38.8481	−120.1	NA	6x	Plastome
I. occidentalis	WCT	6758	California	Eagle Lake	38.94315	−120.123	NA	6X	RADseq
I. occidentalis	JSS	325_a	California	Tamarack lake	38.84517	−120.097	9.5	6x	RADseq
I. occidentalis	JSS	325_b	California	Tamarack lake	38.84517	−120.097	9.6	6x	RADseq
I. occidentalis	JSS	325_c	California	Tamarack lake	38.84517	−120.097	9.7	6x	RADseq
I. occidentalis	JSS	325_d	California	Tamarack lake	38.84517	−120.097	NA	NA	RADseq
I. occidentalis	JSS	331_a	California	Eagle Lake	38.94315	−120.123	9.8	6x	RADseq
I. occidentalis	JSS	331_b	California	Eagle Lake	38.94315	−120.123	9.4	6x	RADseq
I. occidentalis	JSS	340_a	California	Echo lake	38.84562	−120.077	9.8	6x	RADseq
I. occidentalis	JSS	340_b	California	Echo lake	38.84562	−120.077	9.5	6x	RADseq
I. occidentalis	WCT	Grinter-A (G1)	Alaska	Grinter lake	55.97306	−132.762	NA	6x	LFY
I. occidentalis	WCT	Grinter-A (G10)	Alaska	Grinter lake	55.97306	−132.762	NA	6x	RADseq/LFY
I. occidentalis	WCT	Grinter-A (G5)	Alaska	Grinter lake	55.97306	−132.762	NA	6x	LFY
I. occidentalis	WCT	Grinter-A (G7)	Alaska	Grinter lake	55.97306	−132.762	NA	6x	LFY/Plastome
I. aff. hyb. nov. A	WCT	6988	British Columbia	Spider lake	49.34811	−124.627	NA	3x	LFY/Plastome
I. hyb. nov. A	JSS	310	Montana	Twin lakes	45.41283	−113.7	NA	NA	RADseq
I. hyb. nov. A	JSS	342	California	Echo lake	38.84562	−120.077	6.1	4x	RADseq
I. hyb. nov. A	WCT	6759	California	Tamarack lake	38.84517	−120.097	NA	NA	RADseq/Plastome
I. hyb. nov. A	JSS	320_a	California	Tamarack lake	38.84517	−120.097	6	4x	RADseq
I. hyb. nov. A	JSS	320_b	California	Tamarack lake	38.84517	−120.097	5.7	4x	RADseq
I. hyb. nov. A	JSS	332_a	California	Eagle Lake	38.94315	−120.123	6.1	4x	RADseq
I. hyb. nov. A	JSS	332_b	California	Eagle Lake	38.94315	−120.123	6	4x	RADseq
I. hyb. nov. A	JSS	332_c	California	Eagle Lake	38.94315	−120.123	6.1	4x	RADseq
I. hyb. nov. A	JSS	332_d	California	Eagle Lake	38.94315	−120.123	NA	NA	RADseq
I. hyb. nov. A	JSS	332_e	California	Eagle Lake	38.94315	−120.123	6.9	4x	RADseq
I. hyb. nov. B	JSS	341_a	California	Echo lake	38.84562	−120.077	9.9	7x	RADseq
I. hyb. nov. B	JSS	341_b	California	Echo lake	38.84562	−120.077	10.8	7x	RADseq

I. echinospora, *I.* × *herb-wagneri*, *I. maritima*, and *I. occidentalis* which all have well-documented chromosome counts (Britton et al., 1999; Britton and Brunton, 1996, 1993; Taylor, 2002). For plants that we could not identify to a described species, we considered the genome size estimate from flow cytometry along with our other datasets to predict possible ploidy levels and hybrid status.

2.3. Radseq DNA extraction, library preparation, and sequencing

Silica-dried plant tissue samples were supplied to the University of Wisconsin-Madison Biotechnology Center for DNA extractions, library preparation, and sequencing. DNA was extracted using the QIAGEN DNeasy mericon 96 QIAcube HT Kit and quantified using the Quant-iT^{TM} PicoGreen dsDNA kit (Life Technologies, Grand Island, NY).

Libraries were prepared following Elshire et al., (2011) with minimal modification. 100 ng of DNA were digested using PstI and MspI (New

England Biolabs, Ipswich, MA) after which barcoded adapters amenable to Illumina sequencing were added by ligation with T4 ligase (New England Biolabs, Ipswich, MA). The 96 adapter-ligated samples were pooled and amplified to provide library quantities amenable for sequencing, and adapter dimers were removed by SPRI bead purification. The quality and quantity of the finished libraries were assessed using the Agilent Bioanalyzer High Sensitivity Chip (Agilent Technologies, Inc., Santa Clara, CA) and Qubit dsDNA HS Assay Kit (Life Technologies, Grand Island, NY), respectively. Size selection was performed to obtain 300–450 BP fragments. Sequencing was done on Illumina NovaSeq 6000 2 × 150 S2. Images were then analyzed using the standard Illumina Pipeline, version 1.8.2.

2.4. Radseq data processing

All RADseq data processing was done on the Pearse Lab (Utah State University) high-performance workstation; downstream analyses were performed on the University of Utah Center for Higher Performance Computing. Raw data were demultiplexed using the *process_radtags* program in *stacks* v. 2.4 (Catchen et al., 2013, 2011) allowing for a maximum of one mismatch per barcode. Demultiplexed FASTQ files were paired and merged using *ipyrad* v. 0.9.52 (Eaton and Overcast, 2020). Low-quality bases, adapters, and primers were removed from each read. Filtered reads were clustered at 90% similarity, and we required a sequencing depth of six or greater per base, and a minimum of 35 samples per locus to be included in the final assembly. We set a maximum of four unique alleles per locus to account for possible alleles in the polyploid taxa. The *ipyrad* pipeline defines a locus as a short sequence present across samples; from each locus retained in the final assembly *ipyrad* identifies single nucleotide polymorphisms (SNPs). These SNPs are the variation used in our downstream analyses. Since prior hypotheses suspect that the polyploid taxa in this complex are derived from multiple hybridization events and polyploidization events from two original diploid parents, we assumed two possible alleles in diploids, two in tetraploids, and three to four in the hexaploid. In addition to processing all samples together, we partitioned individuals by ploidy (diploids, tetraploids, and hexaploids or higher). The only difference in this approach is that we changed the maximum number of unique alleles per locus for each ploidy group (see above). We recombined the data after this step of the process; in our downstream analyses, we found no difference between data processing methods. Full data processing parameters and downstream analyses can be found on GitHub (github.com/sylviakinosian/isoetes_radSeq).

2.5. Population structure analysis

The program STRUCTURE v. 2.3.4 (Pritchard et al., 2000) estimates admixture between populations of closely related taxa. The program operates with the assumption that each individual's genome is a mosaic from *K* source or ancestral populations. In our analysis, we ran STRUCTURE for $K = 2$–5 with 50 chains for each *K*, with 50,000 generations and a burn-in of 10,000 per chain. We then used CLUMPAK (Kopelman et al., 2015) to process the STRUCTURE output and estimate the best *K* values (Evanno et al., 2005; Pritchard et al., 2000). After viewing the output of STRUCTURE with all samples combined, we reran the program with each combination of putative hybrids and parents. Partitioning data in this manner did not change any of the inferred ancestry relationships among samples. The output from the combined STRUCTURE analysis is provided in the results. To identify the optimal number of populations (K) in our population genomic analysis, we used the "best K" method (Evanno et al., 2005), as well as visually examining $K = 2$–5 as recommended by Pritchard et al. (2000).

2.6. Split network analysis

Split networks display evolutionary relationships among species, as well as conflicting signals in such relationships. They incorporate uncertainty by depicting multiple phylogenetic hypotheses: internal nodes do not represent ancestral taxa, but rather incongruencies between potential evolutionary histories. These conflicting signals indicate where reticulate evolution may be present in the evolutionary history of a group. We utilized the NeighborNet (Bryant and Moulton, 2002) split network algorithm in SplitsTree v. 4.16.1 (Huson and Bryant, 2006). NeighborNet is similar to a neighbor joining tree in that it pairs samples based on similarity, sorting taxa into continually larger groups (Bryant and Moulton, 2002). NeighborNet creates a network where parallel lines indicate splits of taxa, and boxes created by these lines indicate conflicting signals.

2.7. Determination of spore viability

Spores from sequenced individuals were photographed under a Zeiss Discovery v12 instrument (Carl Zeiss Microscopy, LLC, Thornwood, NY, USA). Around half of the individuals from Montana were too immature to have viable spores and were not included. Individual spores were visualized so as to detect any abnormalities that would indicate sterility, such as flattening of the proximal hemisphere, polymorphism, irregularity in size and texture, and connections of meiotic tetrads (Wagner et al., 1986). To determine whether a sample is fertile or sterile megaspores were visualized under a dissecting scope. We followed Wagner et al. (1986) to identify whether spores are spherical, uniform in size, and ornamentation indicating viability and fertility, or flattened, uneven in size and ornamentation indicating non-viability and sterility (Wagner et al., 1986).

2.8. DNA extraction for Illumina and PacBio sequencing

For whole plastome and nuclear allele sequencing, total genomic DNA was isolated from silica dried leaf tissue using the DNeasy Plant Mini Kit (Qiagen Inc., Valencia, CA, USA) at the Smithsonian NMNH Laboratories of Analytical Biology (LAB). Whole genomic DNA was quantified using a Qubit 2.0 fluorometer (ThermoFisher Scientific, Waltham, MA, USA) and quality was measured by 260 nm:280 nm absorption ratio using an Epoch spectrophotometer (BioTek Instruments Inc., Winooski, VT, USA).

2.9. Chloroplast library preparation & sequencing

150–1000 ng of whole genomic DNA was diluted to 60 μL and sheared to ~ 500 BP fragments using the Q800R2 sonicator (Qsonica LLC, Newtown, CT, USA). Fragmented DNA was then prepared for sequencing on a MiSeq Illumina sequencer (Illumina Inc., San Diego, CA, USA) using the NEBNext Ultra II DNA Library Prep Kit for Illumina (New England Biolabs Inc., Ipswich, MA, USA). Manufacturer's instructions were followed for end repair, adaptor ligation, indexing, and PCR enrichment for each sample. Libraries were quantified using a ViiA™ 7 Real-Time PCR System (Applied Biosystems Corp., Foster City, CA, USA). Libraries were then pooled and diluted to 4 nM and submitted for sequencing.

2.10. Chloroplast genome assembly and phylogenetic inference

Illumina's BaseSpace database was used to download index separated raw reads. Pairing, assembling, and referencing the chloroplast reads were done according to Schafran et al. (2018). Adapters and low-quality bases were trimmed using Trimmomatic 0.39, following default settings (Bolger et al. 2004). Paired reads were then mapped to the reference plastome of *Isoëtes flaccida* (Karol et al., 2010) using Bowtie2 (Langmead and Salzberg, 2012), to extract chloroplast reads. The chloroplast reads were then *de novo* assembled using SPAdes 3.10.1 with k-mer lengths 21, 33, 55, 66, 99, and 127 BP (Bankevich et al., 2012). Reference-based assemblies were constructed in Geneious Prime 2.3

(Kearse et al. 2012) by mapping putative chloroplast reads to the *I. flaccida* plastome and extracting the majority consensus sequence. For each sample, *de novo* assembled contigs were aligned to the reference-based assembly and any discrepancies were manually corrected using mapped reads. Assemblies were annotated with GeSeq (Tillich et al. 2017) and combined with annotations from the *I. flaccida* plastome in Geneious. Any discrepancies were resolved by preferring the *I. flaccida* annotations unless contradicted by the nucleotide sequences. Coding sequences that required RNA editing to introduce start codons or stop codons, or remove premature stop codons were assumed to be edited to the same amino acid as the corresponding position in *I. flaccida*. Whole plastomes were aligned with previously sequenced plastomes (Schafran et al., 2018) using MAFFT implemented in Geneious Prime 2.3 and the inverted repeat B region and low complexity repeats were trimmed from the alignment. Phylogenetic inference was done using RAxML 7.3.0 (Stamatakis, 2006) and MrBayes 3.2.6 (Ronquist and Huelsenbeck, 2003). The GTR + G model, with 4000 bootstrap iterations was implemented in RAxML. All MrBayes analyses were run for 50 million generations, under the GTR evolutionary model with gamma-distributed site rate variation, sampling every 1,000 generations, with one cold chain and three heated chains. MCMC output was visualized in Tracer 1.7 to check for convergence among the chains (Rambaut et al., 2018). These computations were run on the FASRC Odyssey cluster supported by the FAS Division of Science Research Computing Group at Harvard University.

2.11. PacBio library preparation for allele sequencing

In preparation for PacBio sequencing of all copies in diploid and polyploid taxa, the second intron of the nuclear gene *LEAFY* (*LFY*) was amplified by the polymerase chain reaction (PCR), using modified 30F (5′-GATCTTTATGAACAATGTGG-3′) and 1190R (5′-GAAATACCTGATTTGTAACC-3′) primers (Frohlich and Meyerowitz 1997; Hoot and Taylor 2001). Amplifications in 25 μL reactions were conducted using the following reagents: 12.5 μL GoTaq (Taq polymerase master mix), 0.5 μL of 0.1 mM BSA (Bovine Serum Albumin), 1 μL of DMSO (Dimethyl Sulfoxide), 1 μL of 10 μM forward and reverse primers, respectively, 6.5 μL of Nuclease free H_2O, and 2.5 μL of DNA. Negative controls and PCR replicates of four suspected polyploids, with the same sample amplified twice by different barcoded primers, were used as quality controls. The PCR protocol began with an initial denaturation temperature of 94℃ for 4 min, 10 cycles of 94℃ for 1 min, 58℃ for 1 min, and 72℃ for 1 min, followed by 25 cycles of 94℃ for 30 s, 53℃ for 1 min, and 72℃ for 30 s; a final extension cycle of 72℃ for 4 min followed. *LFY* amplicons were cleaned using Kapa beads following the manufacturer's protocol (Kapa Biosystems, Wilmington, MA, USA). A 1:1 ratio of bead solution to amplicon was used to remove fragments shorter than the expected 1.1 kb amplicon. The solution was resuspended in 20 μL of nuclease free H_2O. Each cleaned sample was then proportionally pooled, based on concentration and ploidy-level, with other *Isoëtes LFY* amplicons not part of this study and sent to the Duke University Sequencing and Genomic Technologies Shared Resource (Durham, NC) for sequencing using the PacBio RSII platform.

2.12. PacBio data processing and phylogenetic inference

Circular consensus sequences (CCS) provided by the Duke University Sequencing and Genomic Technologies Shared Resource were size filtered to the expected size of the amplicon (1000–1200 bp). We then demultiplexed and clustered the reads in two ways for comparative analysis. First, we demultiplexed and clustered using PURC (Dauphin et al., 2018; Rothfels et al., 2017). Clustering parameters for PURC were set as follows: USEARCH clustering set to 0.997; second clustering set to 0.995; third clustering set to 0.990; final clustering set to 0.997. The size threshold for the minimum number of sequences/clusters was set to 1 and then 4 for the second threshold step. The threshold limit was then set to 10% of the largest cluster for each sample locus. The chimera-killing parameter was set to 1.9. Then, the demultiplexed reads output from PURC were also filtered and clustered by DADA2 (Callahan et al., 2016) to remove those with any "N" base calls and with more than five expected errors. Amplicon sequence variants (ASVs) were identified from the cleaned, demultiplexed reads also using DADA2. Additional details of the pipeline can be found in Schafran (in press). Mock community data show that DADA2 more reliably recovers the true composition of a mixture of amplicon CCS reads compared to OTU clustering, which tends to overestimate the number of taxa present (Nelson et al. 2020a). Therefore, we use only ASVs in downstream analyses. ASVs were aligned to a selection of published *Isoëtes LFY* sequences (Hoot et al., 2004; Rosenthal et al., 2014) using the G-INS-i algorithm in MAFFT V7.313 (Katoh and Standley, 2013). Phylogenies were inferred with IQ-TREE (Nguyen et al., 2015) using the HKY + F model and 1000 ultrafast bootstrap replicates and using MrBayes (Ronquist and Huelsenbeck, 2003) following the parameters described above for chloroplast phylogenetic inference. Topologies were similar between both methods of tree inference, we chose to use the tree output from IQ-TREE.

3. Results

We initially identified all specimens based on morphology, ecology, and distribution (Britton and Brunton, 1996, 1993; Pfeiffer, 1922; Taylor, 2002), although some specimens could not be assigned to a named species or hybrid. Our morphological identifications were compared to our molecular results (plastid, *LFY* nuclear marker, and RADsq data; discussed in detail below), and updated accordingly. Almost all specimens were ultimately identified as named taxa. However, we detected two taxa (with a combination of cytology, molecular data, and examination of spores) that did not match any named species or hybrids. These are hereafter referred to as *Isoëtes* hybrid *novo* A and B.

3.1. Cytology

C-values were only obtained from specimens collected with fresh leaf tissue. For this reason, genome size was not measured for every individual in this study (Table 1). C-values of the diploids, *I. echinospora* and *I. bolanderi,* were smallest. The values of all samples of *I. bolanderi* were between 2.4 and 2.6, while the value for *I. echinospora* was 3.9 (Table 1). Specimens of *I. echinospora* from eastern North America are also known to have a larger C-value compared to other *Isoëtes* diploids, and the genome size of diploid *Isoëtes* species can vary (Bolin et al., 2017). The C-values of tetraploid *I. maritima* ranged from 6.29 to 6.43; hexaploid *I. occidentalis* ranged from 9.4 to 9.8; *I.* hyb. *nov.* A ranged from 5.7 to 6.9; and *I.* hyb. nov. B had values between 9.9 and 10.8 (Table 1). We found that within species, C-values were fairly consistent. The only exception being that we only have one genome size estimate for *I. echinospora* and so cannot speak to intraspecies genome size consistency here; however, this species has been found a consistent diploid by several authors (Kott and Britton, 1980; Britton and Brunton, 1996). In addition, genome size increased with ploidy, with hexaploid *I. occidentalis* having a larger genome than tetraploid *I. maritima*, and both being larger than the diploids in this study. *Isoëtes* hyb. *nov.* A had a genome size range similar to tetraploid *I. maritima*, but smaller than hexploid *I. occidentalis*, indicating it is most likely not a diploid, but probably not a hexaploid. *Isoëtes* hyb. *nov.* B had genome sizes larger than hexploid *I. occidentalis*, suggesting it is at least a hexaploid, likely larger. For both of these putative hybrids, we use C-values as a piece of the puzzle to make inferences about their potential ploidy, and incorporate our other datasets to make hypotheses about their chromosome numbers and hybrid origin. See sections 3.2 and 3.5 for inference of hybrid progenitors.

3.2. Population genomic analysis

Our raw data obtained from the University of Wisconsin-Madison Biotechnology Center consisted of an average of 2.33×10^6 raw reads per sample. In the final assembly, we retained an average of 2,980 loci per sample, with a standard deviation of 858 loci per sample. Our STRUCTURE and SplitsTree analyses utilized a dataset of 3,343 SNPs, composed of one SNP per locus in the final assembly. Raw, demultiplexed sequences can be accessed from the NCBI GenBank Sequence Read Archive (PRJNA665237).

The "best *K*" method (Evanno et al., 2005) indicated a value of 3 as the best fit for our data (Fig. S1), which agreed with our prior morphological and cytological hypotheses on the genomic makeup of these taxa (Fig. 2b). While we understand the issues with assuming the optimal *K* (see Lawson et al., 2018), $K = 3$ was also the most biologically meaningful number of groups because it separated each named diploid, and elucidated parentage in the allopolyploid hybrids. Decreasing *K* below 3 leads to a loss in information and increasing it only adds noise and does not add any meaningful population clusters (Fig. S1).

Our split network (Fig. S2) and population structure (Fig. 2b) analyses showed very similar results. Diploids identified as *I. bolanderi* and *I. echinospora* fall into respective single population groups (Fig. 2b, S2). Putative hybrids including *I* × *herb-wagneri* and *I. maritima* cluster together with half of their genomic constitution coming from *I. echinospora* and *I. bolanderi* (Fig. 2b, S2). Based on population structure analyses, the genomic constitution of *I. maritima* has slightly more *I. echinospora* ancestry than *I. bolanderi* (Fig. 2b), but this could be accounted for by sequencing or analysis errors in the polyploid taxon. All samples of the hexaploid *I. occidentalis* clustered together as a distinct population, without signatures of any other species (Fig. 2b, S2). We recovered a potential hybrid cross between *I. occidentalis* and *I. bolanderi* (*I.* hyb. nov. A). Based on genome size estimates this taxon is likely to be a tetraploid. There was also a heptaploid hybrid between *I. occidentalis* and *I. bolanderi* (*I.* hyb. nov. B; Fig. 2b).

3.3. Determination of spore viability

We determined that most of the spores from *I.* hyb. nov A, B, and *I* × *herb-wagneri* were variable in shape and size, suggesting sterility, while spores from the diploid species (*I. echinospora* and *I. bolanderi*), the tetraploid *I. maritima*, and the hexaploid *I. occidentalis* were uniform in size and shape, suggesting fertility (Fig. 3).

3.4. Whole chloroplast genomes

Bootstrap support as well as posterior probability were high (>95; >0.95) for almost every node in the plastome-derived phylogeny, however this is expected with large sequencing datasets (Fig. 4; Young and Gillung 2020). Three primary clades of interest were recovered: an *I. bolanderi* clade; an *I. echinospora* clade; and an *I. occidentalis* clade. The branch leading to each of these clades has a posterior probability and bootstrap support of 1.00 and 100%, respectively. The *I. echinospora* and *I. occidentalis* clades fall out as sister groups to each other, while the *I. bolanderi* clade is sister to *I. melanopoda* (Fig. 4). Two individuals of *I.* × *herb-wagneri* appear in different places in the phylogeny with one as sister to *I. echinospora*, while the other appears most closely related to *I. bolanderi*, suggesting that each diploid species can be the maternal parent. Individuals identified in the field as *I.* × *pseudotruncata* (Taylor 6988 from Spider lake BC; now regarded as *I.* aff hyb nov. A), as well as the hybrid *I.* hyb. nov. A are most closely related to *I. occidentalis*. No diploid progenitor was found in the *I. occidentalis* clade (Fig. 4).

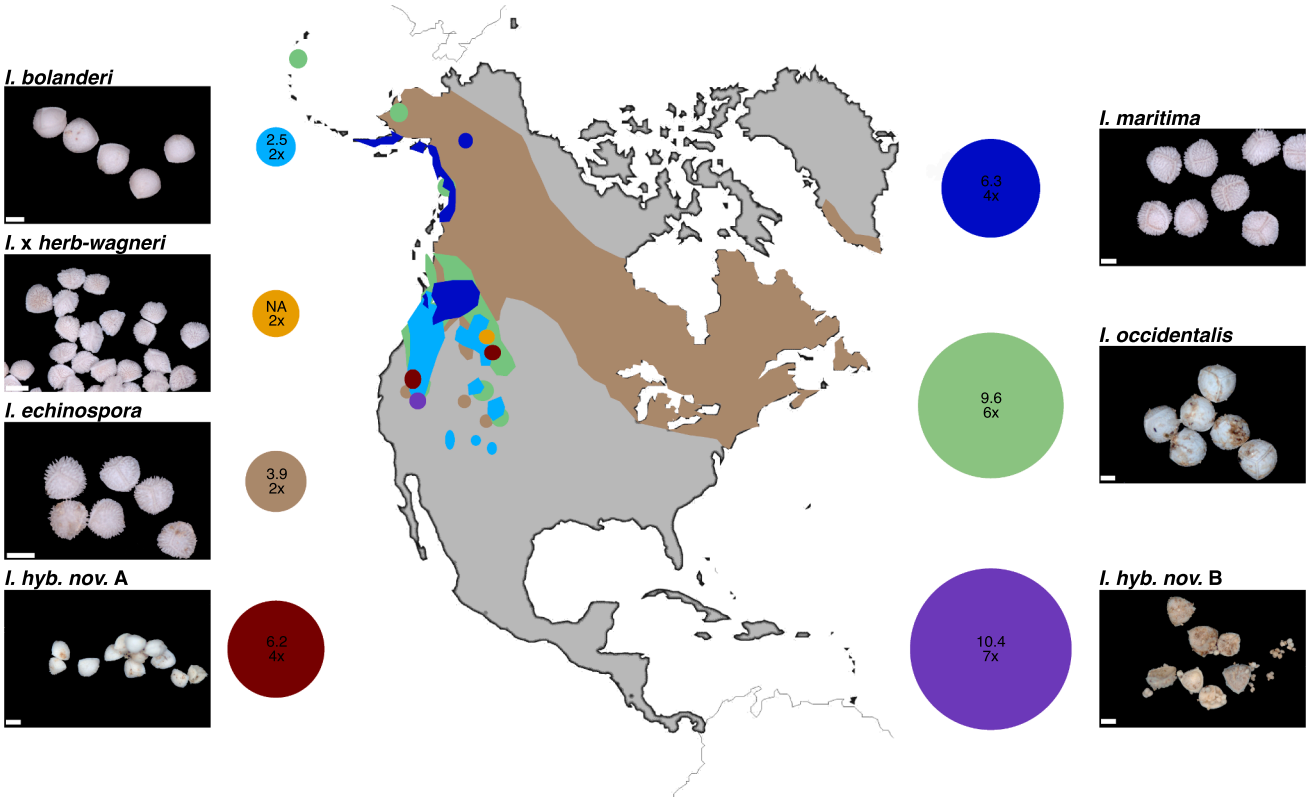

Fig. 3. Spore images depict all sampled species and hybrids. Distribution map of species ranges in North America color coded by taxon. Fertile spores were round and uniform within the sample (*I. bolanderi, I. echinospora, I. maritimata, I. occidentalis*). Sterile spores are misshapen (sometimes flattened) and vary in size sometimes with the meiotic tetrads visible (*I.* × *herb-wagneri*, *I.* hyb. *nov*. A/B). The colored circles that include ploidy level and 1C values for each taxon are sized based on relative 1C values for each depicted taxon and colored based on species. Scale bar on spore images: 200 μm.

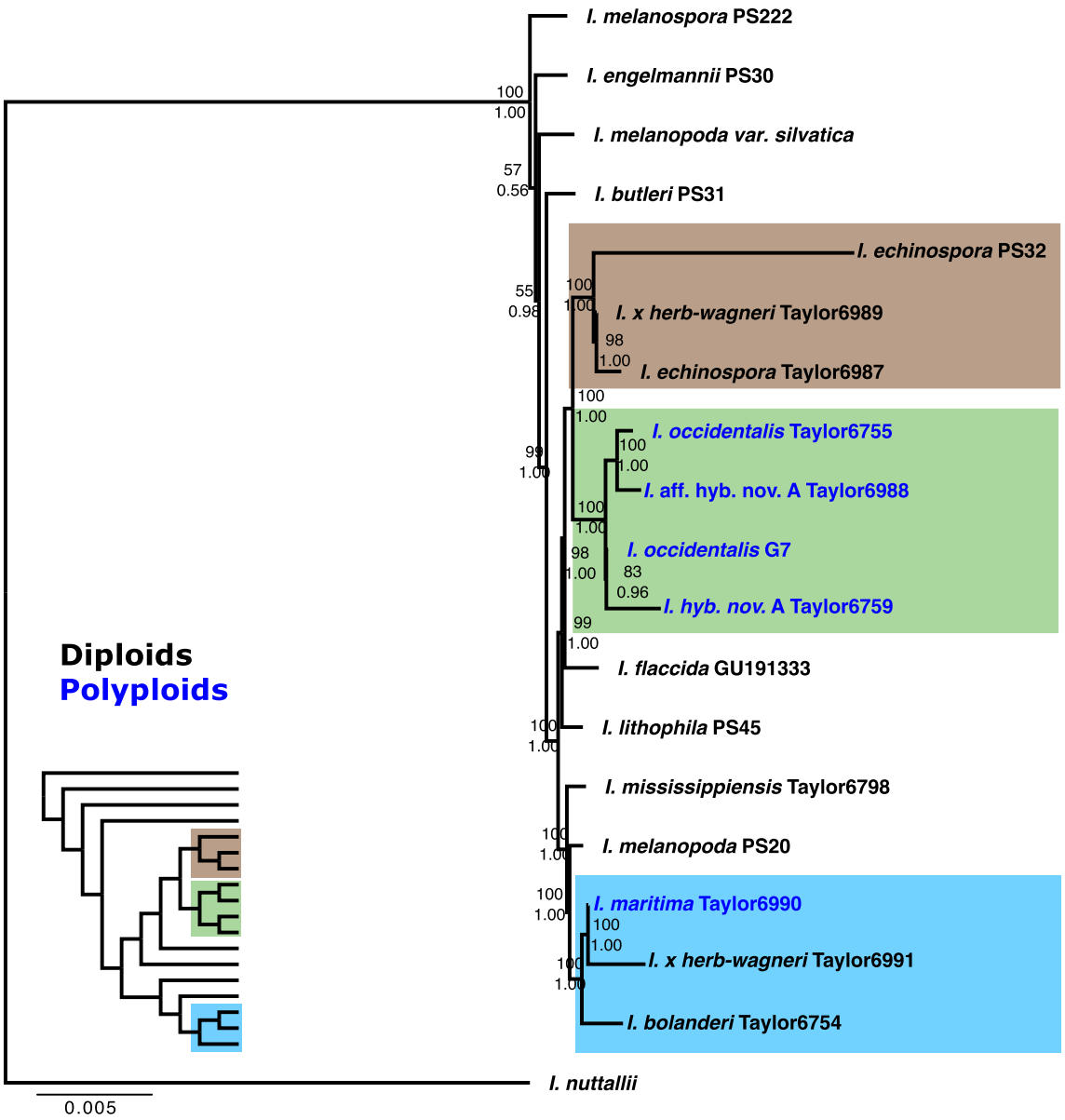

Fig. 4. Plastome phylogeny of western North American *Isoëtes* including outgroups for reference. All individuals in the group of interest comprise three distinct clades: *I. bolanderi* (blue), *I. echinospora* (brown), *I. occidentalis* (green). Within the blue clade, there are accessions of *I. bolanderi*, *I.* × *herb-wagneri*, and *I. maritima*. In the green clade, there are accessions of *I. occidentalis* and *I. hyb. nov.* A. Finally, in the brown clade there are accessions of *I. echinospora*, *I.* × *herb-wagneri*, and *I. maritima*. (For interpretation of the references to color in this figure legend, the reader is referred to the web version of this article.)

3.5. LFY phylogenetic inference

As multiple samples not part of this study were sequenced on the SMRT cell, when we removed sequences not associated with our study taxa we were left with 10,409 CCS reads from PacBio sequencing. 45% of all reads could be demultiplexed or confidently assigned to a sample. Despite efforts to achieve equal sequencing depth, the number of reads per sample ranged from 61 to 1191 (average 548, standard deviation 290). DADA2 inferred a total of 32 ASVs, compared to the 56 OTUs produced with PURC. OTU clustering showed variation in the number of OTUs between three out of four pairs of PCR replicates (multiple replicates of the same sample), while ASVs were identical. Based on a previous demonstration of greater accuracy in mock communities (Nelson et al. 2020a) and greater consistency in our PCR replicates, we used the ASVs for phylogenetic analysis.

The number of ASVs per sample was largely consistent with expectations based on morphological IDs (*i.e.*, basic diploids returned single sequences while diploid hybrids and allopolyploids returned multiple). We found multiple alleles for *I.* × *herb-wagneri*, *I. maritima*, multiple unnamed hybrids, and *I. occidentalis* (Fig. S3). Based on proximity of our *LFY* sequences to reference diploid taxa, there are two different combinations observed. The diploid hybrid *I.* × *herb-wagneri*, its allotetraploid *I. maritima*, and *I.* hyb. nov. A have *LFY* alleles from both putative parent species *I. bolanderi* and *I. echinospora*, while sequences from *I. occidentalis* and *I.* aff. hyb. nov. A are separated in two close sister clades containing diploids *I. echinospora* and *I. prototypus*, respectively. The overall phylogeny contains numerous weakly supported branches. However, this is expected when using a single gene to reconstruct a species tree with extremely closely related taxa (Degnan and Rosenberg, 2009).

4. Discussion

The frequent occurrence of sterile plants with intermediate

morphology, various co-occurring species, and the high proportion of polyploid taxa suggests that reticulate evolution is common in the genus *Isoëtes* (Taylor and Hickey, 1992; Troia et al., 2016). Previous attempts to explain the patterns and evolutionary implications of hybridization and polyploidization in the genus have relied on a single or few genetic markers (Dai et al., 2020; Hoot et al., 2004; Kim et al., 2010; Pereira et al., 2018), which may not accurately depict species relationships in recently diverged groups with low molecular divergence, introgression, and incomplete lineage sorting (Nichols, 2001; Nelson et al. 2020b). With the use of phylogenomic tools including whole plastome sequencing and RADseq, in conjunction with cytological data and information on spore viability, we investigated the importance of hybridization and polyploidization in generating and maintaining novel diversity within a high-ploidy complex of western North American *Isoëtes*.

4.1. Homoploid hybridization and allopolyploidy

The diploid species *Isoëtes bolanderi* and *I. echinospora* co-occur across an extensive portion of the cordilleran region of western North America (Fig. 3). We found that genomic constitution (Fig. 2b, S2, S3), ploidy (Table 1), sterility (Fig. 3), and chloroplast inheritance (Fig. 4), demonstrate that where these species overlap, they hybridize to form the sterile homoploid (diploid) *I.* × *herb-wagneri* (Fig. 5; as initially hypothesized by Taylor, 2002). Since *I.* × *herb-wagneri* is sterile (Fig. 3) it cannot reproduce sexually and—in the absence of asexual reproduction through rootstock division—each individual is the product of a distinct hybridization event. This means that *I.* × *herb-wagneri* cannot persist as a sexually reproducing independent lineage, a necessary step in homoploid hybrid speciation (Yakimowski and Rieseberg, 2014). Based on these data, *Isoëtes bolanderi* and *I. echinospora* are perhaps too evolutionarily divergent (possibly resulting from chromosomal rearrangements or genetic incompatibilities) to form fertile homoploid hybrids, and allopolyploidy must be a necessary step to restore fertility in this system (Buggs et al., 2009). More broadly, it seems that most homoploid hybrids between distinct species in *Isoëtes* are sterile (Taylor and Hickey, 1992), further suggesting that hybridization in the absence of whole genome duplication is unlikely a mechanism of generating novel evolutionarily stable lineages in this group.

Based on overlapping distributions and similar morphology, *Isoëtes maritima* was historically circumscribed as a variety of *I. echinospora* (Löve, 1962). Differences in ploidy later led to the segregation of *I. maritima* as a distinct tetraploid taxon (Brunton and Britton, 1999). The formation of viable spores (Fig. 3), tetraploidy (Table 1), chloroplast inheritance (Fig. 4), and genomic constitution (Fig. 2b, S3) demonstrate that *I. maritima* is the allotetraploid derivative of *I. echinospora* and *I. bolanderi* (Fig. 5). The formation of *I. maritima* may have occurred in multiple ways including the fusion of unreduced gametes in *I.* × *herb-wagneri* or the fusion of unreduced gametes from the diploid parents (*I. echinospora* and *I. bolanderi*). It could have also been formed via a triploid bridge: the fusion of a reduced gamete of one parent with an unreduced gamete of another, followed by a backcross of that triploid hybrid with a reduced gamete from one of the diploid parents (Husband, 2004; Ramsey and Schemske, 2002). Evidence from flowering plants suggests that polyploids and hybrids produce a greater proportion of unreduced gametes than do diploids and non-hybrids (Ramsey and Schemske, 2002), a pattern also observed in *Isoëtes* (Fig. 3; JSS, WCT, and PWS, pers. obs.). This suggests that the first scenario (the fusion of two unreduced gametes of *I.* × *herb-wagneri*) is most likely. Based on the origin of *I. maritima* within this complex, allopolyploidization may be the most likely mechanism of generating novel diversity across hybrid taxa.

4.2. High-ploidy hybrids

In the 1990 s, two sterile hybrids (*Isoëtes* × *pseudotruncata* and *I.* × *truncata*) were documented in northwestern North America (Britton et al., 1999; Britton and Brunton, 1996, 1993). Originally, *Isoëtes* × *pseudotruncata* (3x) was described as the hybrid between *I. maritima* and *I. echinospora*, whereas *I.* × *truncata* (5x) was described as the hybrid between *I. maritima* and *I. occidentalis* (Fig. 1). Our analyses provided limited corroboration for the putative parentage of these hybrids, as described by Britton and Brunton (1993, 1996; Figs. 1, 2b). It is possible that we did not sample these taxa or that their progenitors were misidentified. Interestingly, we did find signatures of two hybrid taxa growing in mixed populations with *I. occidentalis* and *I. bolanderi*

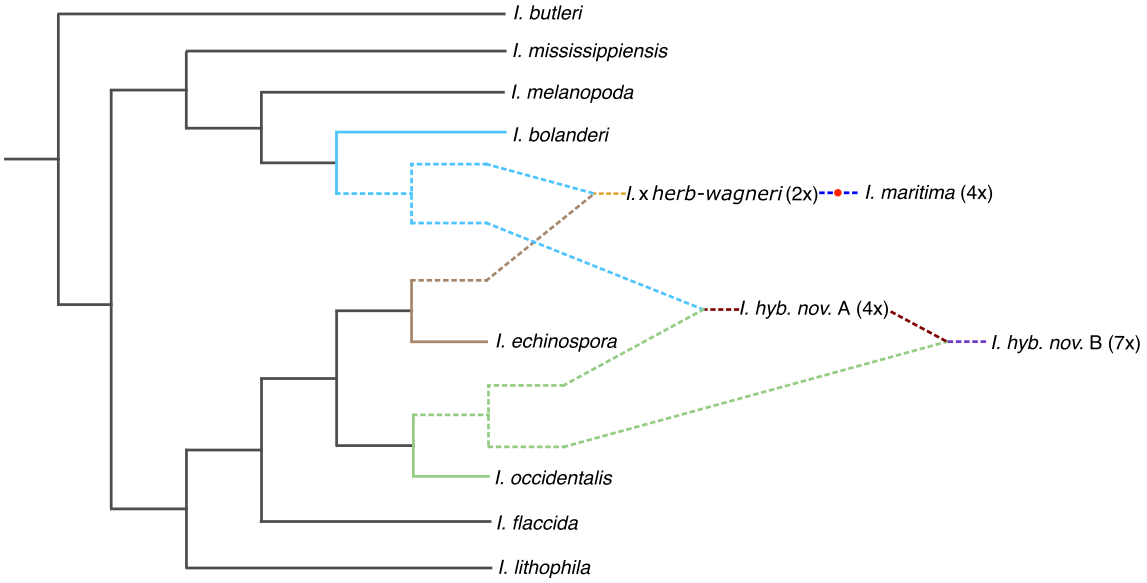

Fig. 5. Hypothesized relationships of western North American *Isoëtes* as supported by this study. *Isoëtes bolanderi* and *I. echinospora* hybridize to form the sterile diploid *I.* × *herb-wagneri*. *Isoëtes maritima* is formed via a whole genome duplication (indicated by red dot) of *I.* × *herb-wagneri*. *Isoëtes bolanderi* (1x gamete) and *I. occidentalis* (3x gamete) hybridize to form the tetraploid *I. hyb. nov.* A. Finally, *I. occidentalis* (3x gamete) and *I. hyb. nov.* A. (4x gamete) hybridize to form the heptaploid *I. hyb. nov.* B. The polyploid origin of *I. occidentalis* is still inconclusive. (For interpretation of the references to color in this figure legend, the reader is referred to the web version of this article.)

(Fig. 2a): *Isoëtes* hyb. *nov.* A and *I.* hyb. *nov.* B (Fig. 2b; Table 1). Both hybrids contain genomic signatures of *I. bolanderi* (or potentially inherited from *I. maritima*) and *I. occidentalis* (Fig. 2b, S2, S3) as well as polymorphic spores, indicating hybrid status and spore sterility (Fig. 3). Given the C-values of these hybrids (Table 1) we suspect that *I.* hyb. *nov.* A is a tetraploid, and *I.* hyb. *nov.* B is a heptaploid. If these are indeed hybrids between their co-occurring species, *I.* hyb. *nov.* A may be a tetraploid derived from a reduced gamete of *I. occidentalis* (3x) and a reduced gamete of *I. bolanderi* (1x). We predict that *I.* hyb. *nov.* B is either the backcross between an unreduced gamete of *I.* hyb. *nov.* A (4x) and *I. occidentalis* (3x) (Fig. 5), or the hybrid product between an unreduced gamete of *I. occidentalis* (6x) and a reduced gamete of *I. bolanderi* (1x).

An important note is that we cannot infer the exact ploidy for *I.* hyb *nov*. A and B because we do not have chromosome counts for these samples. However, we suspect that their ploidy level is odd (3x, 5x, 7x, 9x, etc.) because of their sterility—an established trait of many odd-ploidy hybrids (Hegarty and Hiscock, 2005; Sigel, 2016). It is known that differences in reproductive barriers exist between different levels of interploid hybrids (Sutherland and Galloway, 2017). Based on the presence of various interploid hybrids found in this study, and more broadly in *Isoëtes* (Taylor and Hickey, 1992), these barriers may be weak within the genus, regardless of ploidy level. However, an examination of postzygotic reproductive barriers is needed to fully understand these dynamics. If genome duplication follows hybridization, low prezygotic reproductive barriers may be the mechanism for generating high level interploid hybrid complexes in *Isoëtes*.

Abnormal chromosomal behavior can occur within interploid hybrids (Sigel, 2016). Specifically, chromosomal non-disjunction and uneven chromosomal segmentation can occur during meiosis leading to spores of various ploidy (Sybenga, 1996). In allopolyploid hybrids with highly divergent genomes, homeologous pairing is unlikely, leading to gametes containing only one parent's genomic constitution; if the parental taxa were more closely related, homeologous pairing or crossing over could lead to gametes with a mix of parental genomes (Sybenga, 1996). It is possible that the two interploid hybrids *I.* hyb. *nov.* A and B could produce meiotic products with various cytotypes and genomic constitutions, resulting in pentaploid and triploid taxa like *I.* × *truncata* and *I.* × *pseudotruncata*, respectively. Given this phenomenon, it may be that *I.* × *truncata* and *I.* × *pseudotruncata* are not derived from their initially proposed hybridization events (Fig. 1; Britton and Brunton, 1996, 1993), but rather represent multiple cytotypes derived from abnormal chromosomal behavior of *I.* hyb. *nov.* A and B (Fig. 5). Other lines of evidence may support this, specifically the various spore sizes in these taxa (some large, round and seemingly viable; Fig. 3), and observations that the chloroplast genome of a sterile triploid initially identified as *I.* × *pseudotruncata* (Taylor 6988 Spider Lake, British Columbia, Canada; now named *I.* aff hyb *nov*. A; Fig. 1) is actually derived from *I. occidentalis* (Fig. 4). It is not possible for this taxon to inherit its chloroplast from *I. occidentalis* if it were the hybrid *I.* × *pseudotruncata,* derived from *I. maritima* and *I. echinospora*, as initially hypothesized (Fig. 1; Britton and Brunton, 1993). However, more data including DNA sequences from type species are needed to conclusively determine the genomic identity of *I.* × *pseudotruncata* and *I.* × *truncata*. These interploid hybrids (*I.* hyb. *nov.* A and B) occur in mixed populations in slightly lower densities than their progenitors (JSS, WCT, pers. obs), and also backcross with them, yet are not culled from the population. Based on the shallow divergences of their chloroplast genome and *LFY*, it is possible that these interploid hybrids are so novel that population-level dynamics are still unfolding. Each individual of these interploid hybrids is created by a hybridization event; therefore, in the future, these taxa may naturally go extinct simply due to the fact that no new hybridization events are occurring to produce them.

4.3. Directionality of hybridization events

Because *Isoëtes* is heterosporous, both micro- and megaspores must be present for fertilization to occur. Many of the species in our complex frequently co-occur in these populations, therefore, so do the male and female spores and gametophytes (Fig. 2a). For this reason, one of the main—but not exclusive (Schneller, 1981)—prezygotic barriers should be sperm size and archegonial neck size, due to cell size differences between diploids and polyploids in seed-free plants (Testo et al., 2015). Chloroplast inheritance demonstrates that different individuals of *I.* × *herb-wagneri* have a shared chloroplast lineage with *I. bolanderi* or *I. echinospora*, meaning either parent can be the maternal donor (Fig. 4). Since *I. echinospora* and *I. bolanderi* are diploid, they should have similar sized organs (*i.e.*, sperm, eggs, archegonia), making reciprocal hybridization possible (Haufler et al., 1995; Sigel et al., 2014). In contrast, the hypothesized interploid hybrid *I.* hyb. *nov.* A, is derived from a hexaploid and a diploid (Fig. 2b, 5); with the hexaploid *I. occidentalis* identified as the maternal progenitor (Fig. 4). The directionality of this hybridization event may be due to the sperm size of the hexaploid being larger than the sperm of the diploid (Testo et al., 2015), and the larger hexaploid sperm may not fit down the narrower archegonial neck of the *I. bolanderi* gametophyte. However, there is only one sample indicating the maternal inheritance of *I.* hyb. *nov.* A, and increased sampling may suggest otherwise. While gamete size may be a prezygotic barrier in the directionality of hybridization events, based on the propensity for reproduction between distinct species, and even taxa with various ploidy, there seems to be overall low prezygotic reproductive barriers within the genus, further facilitating hybridization.

4.4. The origin of Isoëtes occidentalis

While morphological variation is documented between northern and southern populations of *Isoëtes occidentalis* (Britton and Brunton, 1993; Pfeiffer, 1922), we found this taxon to be genomically uniform throughout its range (Fig. 2a,b). Using preliminary morphological and ploidy data, we initially hypothesized that *I. occidentalis* was the allohexaploid derivative between reduced gametes of *I. maritima* (which should have one allele from *I. echinospora* and one from *I. bolanderi*) and *I. echinospora* (Fig. 1). If this were the evolutionary history of *I. occidentalis*, the genomic constitution would have signatures of *I. bolanderi* and *I. echinospora* (Fig. 1). We found no sign of this shared ancestry in I. *occidentalis* in either the *LFY* or RADseq data (Fig. S3,2b). While *I. occidentalis* has multiple minimally diverged *LFY* alleles (Fig. S3), none occur in the *I. bolanderi* clade, instead the closest diploids were *I. echinospora* and *I. prototypus*. However, increased sampling density with additional diploids may alter this topology. The presence of a *I. prototypus*-like sequence was unexpected, given it is a rare species of eastern North America (Britton and Goltz, 1991; Taylor et al., 1993). The sister position of *I. prototypus* to our *I. occidentalis* sequences is highly supported, but the short branch lengths separating this clade from *I. echinospora* and other species such as *I. melanopoda* and *I. hawaiiensis* suggest additional low copy nuclear markers may be needed to better resolve this region of the phylogeny. While it is hard to draw a single definitive hypothesis on the origin of *I. occidentalis*, multiple evolutionary histories could lead to these patterns. For instance, *I. occidentalis* could potentially be an autopolyploid, or allopolyploid derived from its originally hypothesized progenitors or extinct/unsampled parents. In our population structure analysis at $K = 2$, we found that *I. occidentalis* has the same genomic constitution as I. *echinospora* (Fig. S1), and our chloroplast (Fig. 4) and nuclear data (Fig. S3) suggest they are close relatives. Our different datasets provide two potential hypotheses for the origin of *I. occidentalis*. Looking at the RADseq data, it is possible that *I. occidentalis* is an autopolyploid of *I. echinospora*. Considering the *LFY* data, *I. occidentalis* may also be an ancient allopolyploid derived from *I. echinospora* and another species, potentially *I. prototypus*. If *I. bolanderi* is a progenitor of *I. occidentalis*, as previously

hypothesized, it could be that enough time has elapsed to allow for genetic divergence and genomic rearrangement (Sigel, 2016), which masks the genomic similarities between these taxa in our data (Fig. 2b). Another possibility is that allelic dropout could have occurred in the RADseq dataset, obscuring the other progenitor of *I. occidentalis*, which is discussed in detail below.

An important consideration regarding our population structure analysis is the disparity in ploidy level across taxa. In its current version, the population genomic analysis program STRUCTURE (v. 2.3.4; Pritchard et al., 2000) cannot process multiple ploidy levels in the same run. *Isoëtes occidentalis* is a hexaploid, and so it is possible that the STRUCTURE is not appropriately dealing with the additional variation within this high-ploidy taxon. This may explain why *I. occidentalis* does not appear to have a significant amount of variation within its genome. However, Stift et al., (2019) showed that among population genomic software, STRUCTURE does the best job accommodating mixed-ploidy in simulated datasets, although this may vary with empirical data. Allelic dropout may also be occurring during sequencing or data processing. RADseq contigs are clustered among samples based on similarity; if *I. occidentalis* contains variation that is absent in the other species we sampled, then novel variation may be lost. In addition, biases in sequences can also cause allelic dropout and missing data. Recently, new sequencing protocols have been developed to mitigate this issue (Cerca et al., 2021; Rivera-Colón et al., 2021). Future work on mixed-ploidy systems in *Isoëtes* will benefit from these advances.

4.5. Biogeographical hypotheses and future direction

Given the distribution of this reticulate complex throughout the Sierra Nevada, Rocky Mountains, and Coast Range, glaciation could have played a role in its evolutionary and biogeographic history (Burnier et al., 2009; Haufler et al., 1995; Jorgensen and Barrington, 2020; Sessa et al., 2012a, 2012b; Stein et al., 2010). Future work should investigate if progenitors of *I. occidentalis* occurred throughout lakes in northwestern North America and whether Quaternary glaciation cycles (Dyke and Prest, 1987; Hughes et al., 1989; Mandryk et al., 2001) led to extinction of the diploid parents, while the polyploid *I. occidentalis* survived in refugia like the 'ice-free corridor' in western Canada (Dyke, 2005; Schweger, 1989). It may be possible that *I. occidentalis* evaded extinction due to a wider distribution and fixed heterozygosity, which buffered populations from inbreeding depression during climatic fluctuations (Brochmann et al., 2004). Similar historical scenarios could be investigated in other high-ploidy species within the genus, such as *I. lacustris* (10x) in eastern North America.

Long-distance dispersal may be another aspect of gene flow and biogeographical patterns in this western North American complex and could be a fruitful area of future research. Anecdotal evidence suggests that *Isoëtes* spores can be dispersed by waterways, waterfowl, or even snails and earthworms (Duthie, 1929; Jermy, 1990; Larsén and Rydin, 2016; Taylor and Hickey, 1992). Recent work has documented spores in waterfowl fecal matter (Silva et al., 2020), confirming previous observations. It is not inconceivable that spores, sporangia, or even whole plants are dispersed in the crops of migratory birds (Les et al., 2003). We suspect that future work may reveal the importance of long-distance dispersal and glaciation cycles on the biogeographical patterns of *Isoëtes*.

5. Conclusion

Understanding the evolutionary implications of polyploidization and hybridization in the generation of biodiversity is a fundamental pillar of biology. Here, we take a step in this direction by determining how these processes affect evolutionary dynamics within a high-ploidy system of the heterosporous lycophyte genus *Isoëtes*. We detected several hybrids and polyploids, their parental origin, and the directionality of hybridization events. Importantly, we found evidence for homoploid hybridization leading to the formation of sterile diploid taxa that undergo whole genome duplication, resulting in fertile polyploid lineages. These newly fertile allopolyploids can hybridize with their diploid progenitors—across ploidy levels—to form sterile interploid hybrids, which then may be able to produce unreduced viable spores continuing this cycle. Interestingly, the directionality of hybridization events is reciprocal between taxa of the same cytotype, but in interploid hybrids, the higher ploidy taxon may act solely as the maternal donor. Finally, we found evidence for a distinct hexaploid lineage mixed signatures of hybrid origin, raising questions about its evolutionary history. Taken together, this suggests that low prezygotic reproductive barriers and a high propensity for polyploidization within *Isoëtes* facilitate the formation of high-ploidy systems and that these processes may be important in the development of new evolutionary lineages and more broadly in shaping extant diversity within the genus.

Declaration of Competing Interest

The authors declare that they have no known competing financial interests or personal relationships that could have appeared to influence the work reported in this paper.

Acknowledgements

We would like to thank William D. Pearse for thoughtful comments on the manuscript. We also thank Gabriel Johnson as well as undergraduate research assistance from Catawba College for help with laboratory procedures and C-value generation. We thank the University of Wisconsin Biotechnology Center DNA Sequencing Facility for providing DNA extraction, library prep, and sequencing facilities and services. We also thank the Weld Hill Research Facility for microscope use. This project was funded in part by The Society of Systematic Biologists Graduate Student Research Grant, awarded to JSS. SPK is funded by a National Science Foundation Graduate Research Fellowship.

Author contributions

Taylor and Zimmer initiated the project, Suissa and Taylor carried out fieldwork, Bolin determined C-values, Suissa and Schafran sequenced and analyzed plastid genomes and *LFY* sequences, Suissa and Kinosian performed RADSeq data processing, Kinosian performed split network and population genomic analyses. All authors participated in writing the manuscript.

Appendix A. Supplementary material

Supplementary data to this article can be found online at https://doi.org/10.1016/j.ympev.2021.107332.

References

Bankevich, A., Nurk, S., Antipov, D., Gurevich, A.A., Dvorkin, M., Kulikov, A.S., Lesin, V. M., Nikolenko, S.I., Pham, S., Prjibelski, A.D., Pyshkin, A.V., Sirotkin, A.V., Vyahhi, N., Tesler, G., Alekseyev, M.A., Pevzner, P.A., 2012. SPAdes: a new genome assembly algorithm and its applications to single-cell sequencing. J. Comput. Biol. 19, 455–477.

Barrington, D.S., Haufler, C.H., Werth, C.R., 1989. Hybridization, reticulation, and species concepts in the ferns. Am. Fern J. 79, 55–64.

Bolger, Anthony M., Lohse, Marc, Usadel, Bjoern, 2014. Trimmomatic: A flexible trimmer for Illumina Sequence Data. Bioinformatics 30 (15), 2114–2120.

Bolin, J.F., Hartwig, C.L., Schafran, P., Komarnytsky, S., 2017. Application of DNA Flow Cytometry to aid species delimitation in *Isoëtes*. Castanea 83, 38–47.

Britton, D.M., Brunton, D.F., 1996. *Isoëtes* × *pseudotruncata*, a new triploid hybrid from western Canada and Alaska. Can. J. Bot. 74, 51–59.

Britton, D.M., Brunton, D.F., 1993. *Isoëtes* × *truncata*: a newly considered pentaploid hybrid from western North America. Can. J. Bot. 71, 1016–1025.

Britton, D.M., Brunton, D.F., 1989. A new *Isoëtes* hybrid (*Isoetes echinospora* × *riparia*) for Canada. Can. J. Bot. 67, 2995–3002.

Britton, D.M., Brunton, D.F., Talbot, S.S., 1999. *Isoëtes* in Alaska and the Aleutians. Am. Fern J. 89, 133–141.

Britton, D.M., Goltz, J.P., 1991. *Isoëtes prototypus*, a new diploid species from eastern Canada. Canadian journal of botany 69, 277–281.

Brochmann, C., Brysting, A.K., Alsos, I.G., Borgen, L., Grundt, H.H., Scheen, A.-C., Elven, R., 2004. Polyploidy in arctic plants. Biol. J. Linn. Soc. Lond. 82, 521–536.
Brunton, D.F., Britton, D.M., 2000. *Isoëtes* ×*echtuckerii*, hyb. *nov*., a new triploid quillwort from northeastern North America. Can. J. Bot. 77, 1662–1668.
Brunton, D.F., Britton, D.M., 1999. Maritime quillwort, Isoëtes maritima (Isoetaceae), in the Yukon territory. Can. Field-Nat. 113, 641–645.
Bryant, D., Moulton, V., 2002. NeighborNet: An agglomerative method for the construction of planar phylogenetic networks. In: Algorithms in Bioinformatics. Springer, Berlin Heidelberg, pp. 375–391.
Buggs, R.J.A., Soltis, P.S., Soltis, D.E., 2009. Does hybridization between divergent progenitors drive whole-genome duplication? Mol. Ecol. 18, 3334–3339.
Burnier, J., Buerki, S., Arrigo, N., Küpfer, P., Alvarez, N., 2009. Genetic structure and evolution of Alpine polyploid complexes: Ranunculus kuepferi (Ranunculaceae) as a case study. Mol. Ecol. 18, 3730–3744.
Callahan, B.J., McMurdie, P.J., Rosen, M.J., Han, A.W., Johnson, A.J.A., Holmes, S.P., 2016. DADA2: High-resolution sample inference from Illumina amplicon data. Nat. Methods 13, 581–583.
Catchen, J., Hohenlohe, P.A., Bassham, S., Amores, A., Cresko, W.A., 2013. Stacks: an analysis tool set for population genomics. Mol. Ecol. 22, 3124–3140.
Catchen, J.M., Amores, A., Hohenlohe, P., Cresko, W., Postlethwait, J.H., 2011. Stacks: building and genotyping loci de novo from short-read sequences. G3 1, 171–182.
Cerca, J., Maurstad, M.F., Rochette, N.C., Rivera-Colón, A.G., Rayamajhi, N., Catchen, J. M., Struck, T.H., 2021. Removing the bad apples: A simple bioinformatic method to improve loci-recovery in de novo RADseq data for non-model organisms. Methods in Ecology and Evolution. 12, 805–817.
Clute, N.W., 1905. What constitutes a species in the genus *Isoëtes*. Fern Bull. 13, 41–47.
Dai, X., Li, X., Huang, Y., Liu, X., 2020. The speciation and adaptation of the polyploids: a case study of the Chinese *Isoëtes* L. diploid-polyploid complex. BMC Evol. Biol. 20, 118.
Dauphin, B., Grant, J.R., Farrar, D.R., Rothfels, C.J., 2018. Rapid allopolyploid radiation of moonwort ferns (*Botrychium*; Ophioglossaceae) revealed by PacBio sequencing of homologous and homeologous nuclear regions. Mol. Phylogenet. Evol. 120, 342–353.
Degnan, J.H., Rosenberg, N.A., 2009. Gene tree discordance, phylogenetic inference and the multispecies coalescent. Trends Ecol. Evol. 24, 332–340.
Dobzhansky, T., 1982. Genetics and the Origin of Species. Columbia University Press.
Dolezel, J., Bartos, J., 2005. Plant DNA flow cytometry and estimation of nuclear genome size. Ann. Bot. 95, 99–110.
Doležel, J., Doleželová, M., Novák, F.J., 1994. Flow cytometric estimation of nuclear DNA amount in diploid bananas (*Musa acuminata* and *M. balbisiana*). Biol. Plant. 36, 351.
Duthie, A.V., 1929. The method of spore dispersal of three South African species of *Isoëtes*. Ann. Bot. os-43, 411–412.
Dyke, A., 2005. Late Quaternary vegetation history of northern North America based on pollen, macrofossil, and faunal remains. Géographie physique et Quaternaire 59, 211–262.
Dyke, A.S., Prest, V.K., 1987. Paleogeography of northern North America, 18000–5000 years ago. Geological Survey of Canada.
Eaton, D.A.R., Overcast, I., 2020. ipyrad: Interactive assembly and analysis of RADseq datasets. Bioinformatics 36, 2592–2594.
Edelman, N.B., Frandsen, P.B., Miyagi, M., Clavijo, B., 2019. Genomic architecture and introgression shape a butterfly radiation. Science 366, 594–599.
Elshire, R.J., Glaubitz, J.C., Sun, Q., Poland, J.A., Kawamoto, K., Buckler, E.S., Mitchell, S.E., 2011. A robust, simple genotyping-by-sequencing (GBS) approach for high diversity species. PLoS One 6, e19379.
Evanno, G., Regnaut, S., Goudet, J., 2005. Detecting the number of clusters of individuals using the software STRUCTURE: a simulation study. Mol. Ecol. 14, 2611–2620.
Freund, F.D., Freyman, W.A., Rothfels, C.J., 2018. Inferring the evolutionary reduction of corm lobation in *Isoëtes* using Bayesian model-averaged ancestral state reconstruction. Am. J. Bot. 105, 275–286.
Frohlich, Michael W., Meyerowitz., Elliot M., 1997. The search for flower homeotic gene homologs in basal angiosperms and Gnetales: a potential new source of data on the evolutionary origin of flowers. Int. J. Plant Sci. 158 (S6), S131–S142.
Grant, V., 1971. Plant Speciation. Columbia University Press.
Greilhuber, J., Doležel, J., Lysak, M.A., Bennett, M.D., 2005. The origin, evolution and proposed stabilization of the terms 'genome size' and 'C-value' to describe nuclear DNA contents. Annals of Botany 95, 255–260.
Haufler, C.H., Pryer, K.M., Schuettpelz, E., Sessa, E.B., Farrar, D.R., Moran, R., Schneller, J.J., Watkins, J.E., Windham, M.D., 2016. Sex and the single gametophyte: Revising the homosporous vascular plant life cycle in light of contemporary research. Bioscience 66, 928–937.
Haufler, C.H., Windham, M.D., Rabe, E.W., 1995. Reticulate evolution in the *Polypodium vulgare* complex. Syst. Bot. 20, 89–109.
Hegarty, M.J., Hiscock, S.J., 2005. Hybrid speciation in plants: New insights from molecular studies. New Phytologist 165, 411–423.
Hickey, R.J., Taylor, W.C., Luebke, N.T., 1989. The species concept in Pteridophyta with special reference to *Isoëtes*. Am. Fern J. 79, 78–89.
Hoot, S.B., Napier, N.S., Taylor, W.C., 2004. Revealing unknown or extinct lineages within *Isoëtes* (Isoetaceae) using DNA sequences from hybrids. Am. J. Bot. 91, 899–904.
Hoot, Sara B., Taylor, W. Carl, 2001. The utility of nuclear ITS, a LEAFY homolog intron, and chloroplast atpB-rbcL spacer region data in phylogenetic analyses and species delimitation in Isoetes. Am. Fern J. 91 (3), 166–177.
Hughes, O.L., Rutter, N.W., Clague, J.J., Fulton, R.J., 1989. Yukon Territory (Quaternary stratigraphy and history. Cordilleran Ice Sheet). Chapter 1, 58–62.
Husband, B.C., 2004. The role of triploid hybrids in the evolutionary dynamics of mixed-ploidy populations. Biol. J. Linn. Soc. Lond. 82, 537–546.
Husband, B.C., Ozimec, B., Martin, S.L., Pollock, L., 2008. Mating consequences of polyploid evolution in flowering plants: current trends and insights from synthetic polyploids. Int. J. Plant Sci. 169, 195–206.
Huson, D.H., Bryant, D., 2006. Application of phylogenetic networks in evolutionary studies. Mol. Biol. Evol. 23, 254–267.
Jermy, A.C., 1990. Isoetaceae. In: Kramer, K.U., Green, P.S. (Eds.), Pteridophytes and Gymnosperms. Springer, Berlin Heidelberg, Berlin, Heidelberg, pp. 26–31.
Jorgensen, S.A., Barrington, D.S., 2020. Two Beringian origins for the allotetraploid fern *Polystichum braunii* (Dryopteridaceae). Syst. Bot. 42, 6–16.
Karol, K.G., Arumuganathan, K., Boore, J.L., Duffy, A.M., Everett, K.D.E., Hall, J.D., Hansen, S.K., Kuehl, J.V., Mandoli, D.F., Mishler, B.D., Olmstead, R.G., Renzaglia, K. S., Wolf, P.G., 2010. Complete plastome sequences of *Equisetum arvense* and *Isoëtes flaccida*: implications for phylogeny and plastid genome evolution of early land plant lineages. BMC Evol. Biol. 10, 321.
Katoh, K., Standley, D.M., 2013. MAFFT multiple sequence alignment software version 7: improvements in performance and usability. Mol. Biol. Evol. 30, 772–780.
Kearse, M., Moir, R., Wilson, A., Stones-Havas, S., Cheung, M., Sturrock, S., Buxton, S., Cooper, A., Markowitz, S., Duran, C., Thierer, T., Ashton, B., Meintjes, P., Drummond, A., 2012. Geneious Basic: an integrated and extendable desktop software platform for the organization and analysis of sequence data. Bioinformatics 28, 1647–1649.
Kim, C., Shin, H., Chang, Y.-T., Choi, H.-K., 2010. Speciation pathway of *Isoëtes* (Isoëtaceae) in East Asia inferred from molecular phylogenetic relationships. Am. J. Bot. 97, 958–969.
Klekowski, E.J., 1976. Homoeologous chromosome pairing in ferns. Curr. Chrom. Res. 175–184.
Kopelman, N.M., Mayzel, J., Jakobsson, M., Rosenberg, N.A., Mayrose, I., 2015. Clumpak: a program for identifying clustering modes and packaging population structure inferences across K. Mol. Ecol. Resour. 15, 1179–1191.
Kott, L.S., Britton, D.M., 1980. Chromosome numbers for Isoëtes in northeastern North America. Can. J. of Bot. 58, 980–984.
Landis, J.B., Soltis, D.E., Li, Z., Marx, H.E., Barker, M.S., Tank, D.C., Soltis, P.S., 2018. Impact of whole-genome duplication events on diversification rates in angiosperms. Am. J. Bot. 105, 348–363.
Langmead, B., Salzberg, S.L., 2012. Fast gapped-read alignment with Bowtie 2. Nat. Methods 9, 357–359.
Larsén, E., Rydin, C., 2016. Disentangling the phylogeny of *Isoëtes* (Isoetales), using nuclear and plastid data. Int. J. Plant Sci. 177, 157–174.
Lawson, D.J., van Dorp, L., Falush, D., 2018. A tutorial on how not to over-interpret STRUCTURE and ADMIXTURE bar plots. Nat. Commun. 9, 3258.
Les, D.H., Crawford, D.J., Kimball, R.T., Moody, M.L., Landolt, E., 2003. Biogeography of discontinuously distributed hydrophytes: A molecular appraisal of intercontinental disjunctions. Int. J. Plant Sci. 164, 917–932.
Linder, C.R., Rieseberg, L.H., 2004. Reconstructing patterns of reticulate evolution in plants. Am. J. Bot. 91, 1700–1708.
Löve, Á., 1962. Cytotaxonomy of the *Isoëtes echinospora* Complex. Am. Fern J. 52, 113–123.
Mandryk, C.A.S., Josenhans, H., Fedje, D.W., 2001. Late Quaternary paleoenvironments of Northwestern North America: implications for inland versus coastal migration routes. Quat. Sci. Rev. 20, 301–314.
Mayrose, I., Zhan, S.H., Rothfels, C.J., Arrigo, N., Barker, M.S., Rieseberg, L.H., Otto, S. P., 2015. Methods for studying polyploid diversification and the dead end hypothesis: a reply to Soltis et al. (2014). New Phytol. 206, 27–35.
Mayrose, I., Zhan, S.H., Rothfels, C.J., Magnuson-Ford, K., Barker, M.S., Rieseberg, L.H., Otto, S.P., 2011. Recently formed polyploid plants diversify at lower rates. Science 333, 1257.
Nakhleh, L., Warnow, T., Linder, C.R., 2005. Reconstructing reticulate evolution in species—theory and practice. Journal of Computational Biol. 12, 796–811.
Nauheimer, L., Cui, L., Clarke, C., Crayn, D.M., Bourke, G., Nargar, K., 2019. Genome skimming provides well resolved plastid and nuclear phylogenies, showing patterns of deep reticulate evolution in the tropical carnivorous plant genus *Nepenthes* (Caryophyllales). Aust. Syst. Bot. 32, 243–254.
Nelson, J.M., Hauser, D.A., Li, F.W., 2020. Symbiotic cyanobacteria communities in hornworts across time, space, and host species. bioRxiv. https://doi.org/2020.06.18.160382.
Nelson, T.C., Stathos, A.M., Vanderpool, D.D., Finseth, F.R., Yuan, Y.-W., Fishman, L., 2020. Ancient and recent introgression shape the evolutionary history of pollinator adaptation and speciation in a model monkeyflower radiation (*Mimulus* section Erythranthe). bioRxiv. https://doi.org/10.1101/2020.09.08.287151.
Nguyen, L.T., Schmidt, H.A., Von Haeseler, A., Minh, B.Q., 2015. IQ-TREE: a fast and effective stochastic algorithm for estimating maximum-likelihood phylogenies. Molecular biology and evolution 32, 268–274.
Nichols, R., 2001. Gene trees and species trees are not the same. Trends in Ecology & Evolution 16, 358–364.
Pereira, J., Labiak, P.H., Stützel, T., 2017. Origin and biogeography of the ancient genus *Isoëtes* with focus on the Neotropics. Bot. J. Linn. Soc. 185, 253–271.
Pereira, J., Labiak, P.H., Stützel, T., Schulz, C., 2018. Nuclear multi-locus phylogenetic inferences of polyploid *Isoëtes* species (Isoëtaceae) suggest several unknown diploid progenitors and a new polyploid species from South America. Bot. J. Linn. Soc. 189, 6–22.
Pfeiffer, N.E., 1922. Monograph of the Isoetaceae. Ann. Mo. Bot. Gard. 9, 79–233.
Pigg, K.B., 1992. Evolution of isoetalean lycopsids. Ann. Mo. Bot. Gard. 79, 589–612.
Pritchard, J.K., Stephens, M., Donnelly, P., 2000. Inference of population structure using multilocus genotype data. Genetics 155, 945–959.

Rambaut, A., Drummond, A.J., Xie, D., Baele, G., Suchard, M.A., 2018. Posterior summarization in Bayesian phylogenetics sing Tracer 1.7. Syst. Biol. 67, 901–904.
Ramsey, J., Schemske, D.W., 2002. Neopolyploidy in flowering plants. Annu. Rev. Ecol. Syst. 33, 589–639.
Rieseberg, L.H., 1997. Hybrid origins of plant species. Annu. Rev. Ecol. Syst. 28, 359–389.
Rivera-Colón, A.G., Rochette, N.C., Catchen, J.M., 2021. Simulation with RADinitio improves RADseq experimental design and sheds light on sources of missing data. Molecular Ecology Resources 21, 363–378.
Ronquist, F., Huelsenbeck, J.P., 2003. MrBayes 3: Bayesian phylogenetic inference under mixed models. Bioinformatics 19, 1572–1574.
Rosenthal, M.A., Rosenthal, S.R., Johnson, G., Taylor, W.C., Zimmer, E.A., 2014. *Isoëtes viridimontana*: a previously unrecognized quillwort from Vermont, USA. Am. Fern J. 104, 7–15.
Rothfels, C.J., Pryer, K.M., Li, F.-W., 2017. Next-generation polyploid phylogenetics: Rapid resolution of hybrid polyploid complexes using PacBio single-molecule sequencing. New Phytol. 213, 413–429.
Sandstedt, G.D., Wu, C.A., Sweigart, A.L., 2020. Evolution of multiple postzygotic barriers between species of the *Mimulus tilingii* complex. BioRxiv. https://doi.org/10.1101/2020.08.07.241489.
Schafran, P.W., Li, F.-W., Rothfels, C.J. In press. PURC v2.0: a program for improved sequence inference for polyploid phylogenetics and other manifestations of the multiple-copy problem. In: Van de Peer, Y. (ed.) Polyploidy: Methods and Protocols. Methods in Molecular Biology. Springer, New York, NY.
Schafran, P.W., Zimmer, E.A., Taylor, W.C., Musselman, L.J., 2018. A whole chloroplast genome phylogeny of diploid species of *Isoëtes* (Isoetaceae, Lycopodiophyta) in the southeastern United States. Castanea 83, 224–235.
Schneller, J.J., 1981. Evidence for intergeneric incompatibility in ferns. Plant Syst. Evol. 137, 45–56.
Schweger, C.E., 1989. Paleoecology of the western Canadian ice-free corridor. Quaternary geology of the Canadian Cordillera; Quaternary geology of Canada and Greenland. Edited by RJ Fulton. Geological Survey of Canada, Geology of Canada 1, 491–498.
Sessa, E.B., Zimmer, E.A., Givnish, T.J., 2012a. Reticulate evolution on a global scale: a nuclear phylogeny for New World *Dryopteris* (Dryopteridaceae). Mol. Phylogenet. Evol. 64, 563–581.
Sessa, E.B., Zimmer, E.A., Givnish, T.J., 2012b. Unraveling reticulate evolution in North American *Dryopteris* (Dryopteridaceae). BMC Evol. Biol. 12, 104.
Sigel, E.M., 2016. Genetic and genomic aspects of hybridization in ferns. J. Syst. Evol. 54, 638–655.
Sigel, E.M., Windham, M.D., Pryer, K.M., 2014. Evidence for reciprocal origins in *Polypodium hesperium* (Polypodiaceae): a fern model system for investigating how multiple origins shape allopolyploid genomes. Am. J. Bot. 101, 1476–1485.
Silva, G.G., Green, A.J., Hoffman, P., Weber, V., 2020. Seed dispersal by neotropical waterfowl depends on bird species and seasonality. Freshwater Biology 65, 1–11.
Small, R.L., Hickey, R.J., 2001. Systematics of the Northern Andean *Isoëtes karstenii* Complex. Am. Fern J. 91, 41–69.
Soltis, D.E., Segovia-Salcedo, M.C., Jordon-Thaden, I., Majure, L., Miles, N.M., Mavrodiev, E.V., Mei, W., Cortez, M.B., Soltis, P.S., Gitzendanner, M.A., 2014. Are polyploids really evolutionary dead-ends (again)? A critical reappraisal of Mayrose et al.(2011). New Phytol. 202, 1105–1117.
Soltis, P.S., Soltis, D.E., 2000. The role of genetic and genomic attributes in the success of polyploids. Proc. Natl. Acad. Sci. U. S. A. 97, 7051–7057.
Stamatakis, A., 2006. RAxML-VI-HPC: maximum likelihood-based phylogenetic analyses with thousands of taxa and mixed models. Bioinformatics 22, 2688–2690.
Stebbins, G.L., 1969. The significance of hybridization for plant taxonomy and evolution. Taxon 18, 26–35.
Stebbins Jr, G.L., 1947. Types of polyploids; their classification and significance. Adv. Genet. 1, 403–429.
Stein, D.B., Hutton, C., Conant, D.S., Haufler, C.H., Werth, C.R., 2010. Reconstructing *Dryopteris* "semicristata" (Dryopteridaceae): Molecular profiles of tetraploids verify their undiscovered diploid ancestor. Am. J. Bot. 97, 998–1004.
Stift, M., Filip, K., Meirmans, P.G., 2019. Structure is more robust than other clustering methods in simulated mixed-ploidy populations. Heredity 123, 429–441.
Sutherland, B.L., Galloway, L.F., 2017. Postzygotic isolation varies by ploidy level within a polyploid complex. New Phytol. 213, 404–412.
Sybenga, J., 1996. Chromosome pairing affinity and quadrivalent formation in polyploids: do segmental allopolyploids exist? Genome 39, 1176–1184.
Taylor, W.C., 2002. *Isoëtes*×*herb-wagneri*, an interspecific hybrid of *I. bolanderi*× *I. echinospora* (Isoëtaceae). Am. Fern J. 92, 161–163.
Taylor, W.C., Hickey, R.J., 1992. Habitat, evolution, and speciation in Isoëtes. Ann. Mo. Bot. Gard. 79, 613–622.
Taylor, W.C., Luebke, N.T., 1988. *Isoëtes*× *hickeyi*: A naturally occurring hybrid between I. echinospora and I. macrospora. Am. Fern J. 78, 6–13.
Taylor, W.C., Luebke, N.T., Britton, D.M., Hickey, R.J., Brunton, D.F., 1993. Isoëtaceae. In: Editorial Committee, F.N.A. (Ed.), Flora of North America, North of Mexico, vol. 2. Oxford University Press, New York, New York, pp. 64–75.
Testo, W.L., Watkins Jr, J.E., Barrington, D.S., 2015. Dynamics of asymmetrical hybridization in North American wood ferns: reconciling patterns of inheritance with gametophyte reproductive biology. New Phytol. 206, 785–795.
Tillich, M., Lehwark, P., Pellizzer, T., Ulbricht-Jones, E.S., Fischer, A., Bock, R., Greiner, S., 2017. GeSeq – versatile and accurate annotation of organelle genomes. Nucleic Acids Research 45 (W1), W6–W11. https://doi.org/10.1093/nar/gkx391.
Troia, A., Pereira, J.B., Kim, C., Taylor, W.C., 2016. The genus *Isoëtes* (Isoetaceae): a provisional checklist of the accepted and unresolved taxa. Phytotaxa 277, 101–145.
Wagner Jr, W.H., Wagner, F.S., 1980. Polyploidy in pteridophytes. Basic Life Sci. 13, 199–214.
Wagner, W.H., Wagner, F.S., Taylor, W.C., 1986. Detecting abortive spores in herbarium specimens of sterile hybrids. Am. Fern J. 76, 129–140.
Wood, D., Besnard, G., Beerling, D.J., Osborne, C.P., Christin, P.-A., 2020. Phylogenomics indicates the "living fossil" *Isoëtes* diversified in the Cenozoic. PLoS One 15, e0227525.
Wood, T.E., Takebayashi, N., Barker, M.S., Mayrose, I., Greenspoon, P.B., Rieseberg, L. H., 2009. The frequency of polyploid speciation in vascular plants. Proc. Natl. Acad. Sci. U. S. A. 106, 13875–13879.
Yakimowski, S.B., Rieseberg, L.H., 2014. The role of homoploid hybridization in evolution: a century of studies synthesizing genetics and ecology. Am. J. Bot. 101, 1247–1258.
Young, A.D., Gillung, J.P., 2020. Phylogenomics—principles, opportunities and pitfalls of big-data phylogenetics. Systematic Entomology. 45, 225–247.